Int. J. Electrochem. Sci., 14 **(2019)** 4318 – 4326, doi: 10.20964/2019.05.14

International Journal of
ELECTROCHEMICAL
SCIENCE
www.electrochemsci.org

Short Communication

Correlation between Magnetic Properties and Corrosion Resistance of $SmCo_5$/α-Fe Nanocomposite Magnet

Qiong Wu[*], *Jinting Li, Pengyue Zhang, Minxiang Pan*[*], *Hongliang Ge*

Magnetism key laboratory of Zhejiang Province, China Jiliang University, Hangzhou 310018, China
[*]E-mail: wuqiong@cjlu.edu.cn (Qiong Wu); panminxiang@cjlu.edu.cn (Minxiang Pan)

Received: 8 Janary 2019 / *Accepted:* 17 February 2019 / *Published:* 10 April 2019

The exchange-coupled $SmCo_5$/α-Fe nanocomposite magnets were fabricated by the micrometer sized of $SmCo_5$ and α-Fe powders. The effect of α-Fe content on the microstructure, magnetic properties and corrosion resistance of these nanocomposite magnets were systematically discussed. The results revealed that show the enhanced exchange-coupling behavior with $(BH)_{max}$ = 11.3 kJ/m^3 was obtained with the α-Fe content at 7.5 wt%. The magnetization reversal behavior and exchange coupling effect were investigated by analyzing recoil loops and δm -plots, it shows that the exchange coupling interaction is enhanced and finally enhancing the magnetic properties with α-Fe added. Besides, a remarkably improvement in electrochemical stability and corrosion resistance for the $SmCo_5$/α-Fe nanocomposite magnet with the α-Fe added, which is mainly attributed to the coexistence of hard and soft magnetic phases in the magnet.

Keywords: $SmCo_5$/α-Fe; Corrosion; Magnetic properties; Magnetization behavior

1. INTRODUCTION

In recent years, due to the application of high-end magnetic technology in new science and technology fields, such as computer, information storage, biomedicine and micro-nano machinery, the research of nanocrystalline permanent magnet has attracted much attention[1-3]. However, due to the superparamagnetic effect, the coercivity of general permanent magnets decreases significantly at nanoscale. Only high magnetocrystalline anisotropic materials such as SmCo can maintain certain coercivity, especially as $SmCo_5$ magnet has high magnetocrystalline anisotropy constant K_u (2.3×10^8 erg/cm^3), so its superparamagnetic limit is the smallest, which is the ideal material for preparing nanocrystalline permanent magnet material[4,5]. Although nanocrystalline magnet has been extensively studied, the maximum energy product $(BH)_{max}$ of nanocrystalline permanent magnets prepared in practice is far lower than that predicted in theory, which is mainly due to the fact that

microstructures of materials prepared at present are far from the requirements of ideal models. Recent studies showed that the exchange-coupled $SmCo_5$/α-Fe nanocomposite alloys show an important class of high performance magnets, as the $SmCo_5$ hard magnetic phase obtaining high coercivity (H_{cj}) and high Curie temperature (T_c), α-Fe soft magnetic phase obtaining high saturation magnetization (M_s)[6-8]. However, it is still challenging to simultaneously gain in uniform orientation of magnetization vectors for soft and hard magnetic phases in the nanocomposite magnets.

In order to further enhance the magnetic properties and refine the microstructure of the $SmCo_5$/α-Fe nanocomposite magnets, the effect of soft magnetic α-Fe phase content on the magnetic properties, microstructures, magnetization behavior and corrosion resistance of the $SmCo_5$/α-Fe nanocomposite alloys were systematically investigated.

2. EXPERIMENTAL PART

The $SmCo_5$ ingot was prepared by threefold arc melting with high purity metals (≥99.99 %). The $SmCo_5$ ingot was then ground into powder size of ~300 μm and mixed with commercial iron powders with a particle size of ~ 15 μm. The two-phase powders were milled for 2 h by the high-energy ball milling with α-Fe weight ratios at 0 wt. %, 2.5 wt. %, 5 wt. %, and 7.5 wt. %. The as-milled $SmCo_5$/α-Fe powders were pressed into cubes under argon atmosphere, then pressed in the cold isostatic with the pressure of 100 MPa.

The phase structures of $SmCo_5$/α-Fe magnets were characterized by X-ray diffraction (XRD). The magnetic properties and magnetization reversal process of the samples were measured by the vibrating-sample magnetometer (VSM, Lakeshore 7407) with the magnetic field of 2.0 T. The polarization curves were measured by the electrochemical workstation (PARSTAT 2273) under 2.5 wt.% NaCl aqueous solution with a scan rate of 2 mV/s. The accelerated corrosion test was performed by placing samples (cylindrical: Φ5*5 mm) in 120℃, 2 bar and 100% relative humid atmosphere for 24, 48, 72 and 96 h, respectively.

3. RESULTS AND DISCUSSION

Fig. 1 shows the X-ray diffraction patterns of the $SmCo_5$/α-Fe nanocomposite magnets with different α-Fe contents. It is shown that the dominant phase in the single $SmCo_5$ alloy (Fig. 1(a)) is $CaCu_5$-type $SmCo_5$ phase. By the comparison of all the XRD patterns of the $SmCo_5$/α-Fe nanocomposite magnets with different α-Fe contents, it is shown that with increase of α-Fe content from 2.5% to 5.0%, the intensity of diffractions for the $SmCo_5$/α-Fe magnets were reduced, then the width of diffraction peak was broadened. Meanwhile, the influence of soft magnetic α-Fe phase addition on the single-crystal $SmCo_5$ hard magnetic phase is not obvious.

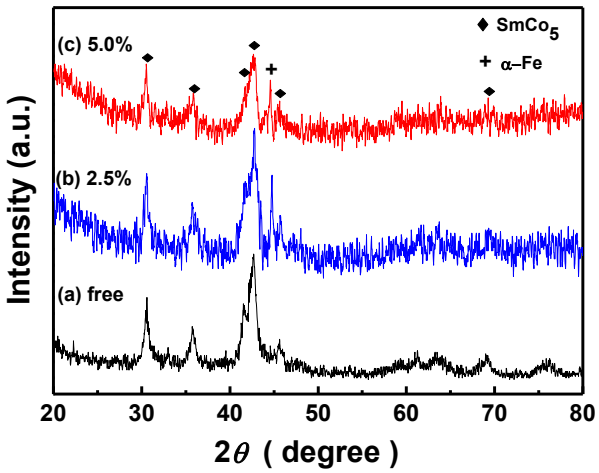

Figure 1. X-ray diffraction patterns of the $SmCo_5$/α-Fe nanocomposite magnets with different α-Fe contents.

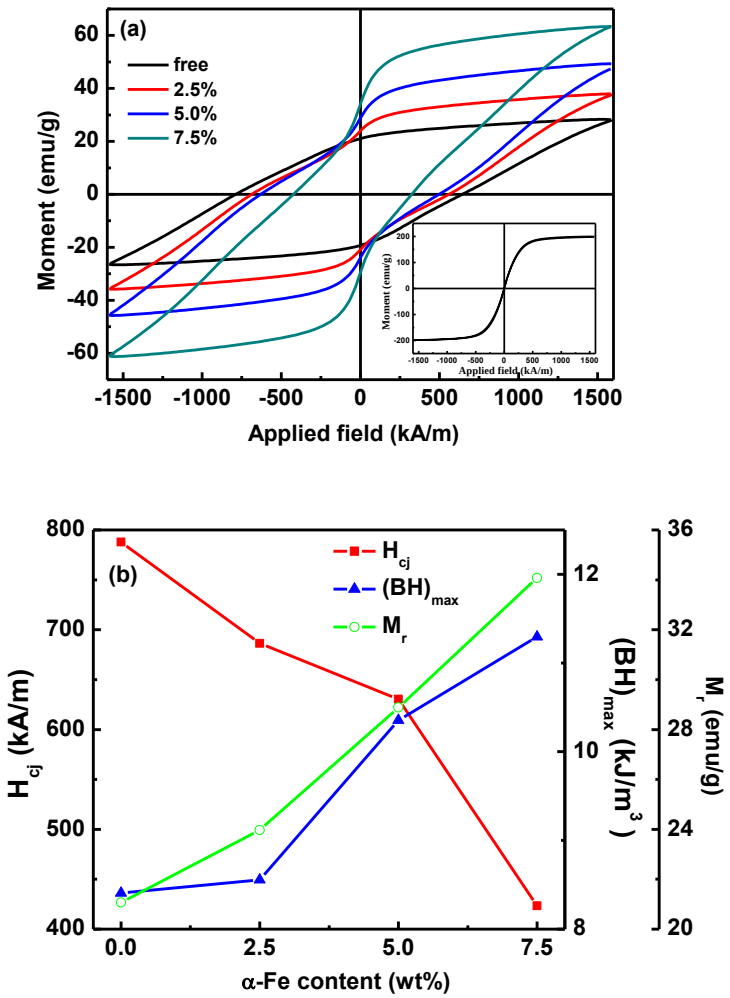

Figure 2. (a) Hysteresis loops of the $SmCo_5$/α-Fe nanocomposite powders with different α-Fe contents. Inset: the hysteresis loop of the original pure α-Fe powders was also shown. (b) Parameters of H_{cj}, $(BH)_{max}$, and M_r for the $SmCo_5$/α-Fe nanocomposite alloys as a function of different α-Fe contents.

The above result revealed the fact that the microstructure for the $CaCu_5$-type $SmCo_5$ phase could be refined. The similar behavior of α-Fe addition for SmCo alloys has been reported by Feng et al. previously [9]. According to the Scherrer's formula, the average grain size of the hard and soft phase for the $SmCo_5$/α-Fe nanocomposite magnets as a function of different α-Fe contents was close to 20 nm.

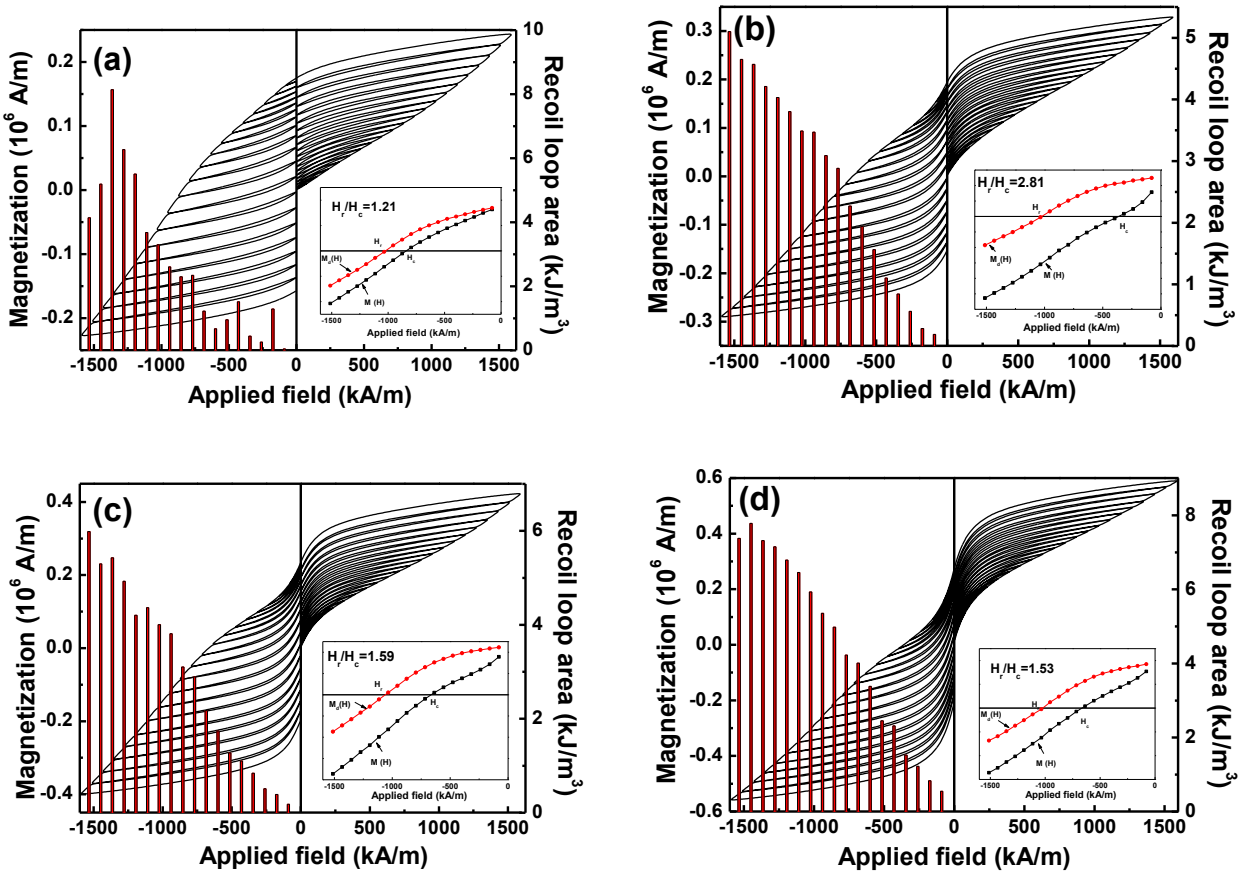

Figure 3. Recoil loops and integrated recoil loop area (vertical bars) of the demagnetization curves on the applied reversal field of the $SmCo_5$/α-Fe nanocomposite magnets for the α-Fe content at (a) free, (b) 2.5 wt%, (c) 5.0 wt%, and (d) 7.5 wt%. The plots of $M(H)$ and $M_d(H)$ are given in the inset also.

Fig. 2 (a) presents the hysteresis loops of $SmCo_5$/α-Fe nanocomposite alloys with different α-Fe contents. The hysteresis loop of the original pure α-Fe powders was also shown in the inset, it has high saturation (M_s: 199.8 emu/g) and low coercivity (H_{cj}: 2.5 kA/m). As shown in Fig 2. (a), the coercivity of α-Fe addition nanocomposite magnets are lower than the α-Fe free sample (H_{cj}: 787.9 kA/m), implying that the magnetic properties of the nanocomposite magnets are sensitive to the different ratio of the hard $SmCo_5$ and soft α-Fe phases, reflecting the existence of the exchange-coupling interaction in these $SmCo_5$/α-Fe nanocomposite alloys. Meanwhile, Fig. 2 (b) gives more information about parameters of H_{cj}, $(BH)_{max}$, and M_r for the $SmCo_5$/α-Fe nanocomposite alloys as a function of different α-Fe contents. It is shown that the coercivity (H_{cj}) decreased monotonically with the increase of α-Fe content, while the $(BH)_{max}$ and M_r show the tendency that is increased

monotonically. The increase of the remanence (M_r) could be due to the fact that the random diffusion of α-Fe into $SmCo_5$ initiated during ball milling process, similar results were also reported by Saravanan et al. [10] for their $SmCo_5$/Fe nanocomposite magnets. The optimal magnetic properties were obtained for the α-Fe content at 7.5 wt%: H_{cj}=423.3 kA/m, M_r =34.1 emu/g, $(BH)_{max}$=11.3 kJ/m^3. Compared to the α-Fe free sample, the maximum energy product $(BH)_{max}$ can get 35% improvements.

To get further understand the effect of α-Fe content on the magnetic behavior of these nanocomposite magnets, the magnetization mechanism of the $SmCo_5$/α-Fe nanocomposite alloys is discussed as follows. Figs. 3 (a) - (d) display the recoil loops for the $SmCo_5$/α-Fe nanocomposite magnets with different α-Fe contents. As seen, the recoil loops for all samples do not close, while the slope of recoil loops is gradually steeper with more α-Fe content, demonstrating that the enhanced exchange-coupling interaction was obtained in the α-Fe addition alloys, compared to the α-Fe free sample. Such a behavior that the open and steeper slope of the recoil loop is considered to be the presence of the exchange-mechanism [11,12], which is mainly due to the exchange coupling interaction between the $SmCo_5$ and α-Fe phase. Similar behavior was also reported previously in the α-Fe/$Nd_2Fe_{14}B$[13], α-Fe/$Sm_2Fe_{14}Cu_{0.5}Ga_2C_2$[14], and $SmCo_7$[15] alloys. Additionally, the enclosed area of the recoil loop is equivalent to the energy loss after one cycle. Vertical bars represent recoil loop areas, as it can be seen the recoil area in Figs. 3 that the maximum value of the area enclosed by a single recoil loop for the α-Fe content magnets (5.27, 5.98, and 7.38 kJ/m^3 for 2.5, 5, 7.5 wt% α-Fe, respectively) are lower than the α-Fe free sample (8.14 kJ/m^3).It can be concluded that the α-Fe doped samples show lower energy losses as a function of the reversal field is applied, although the magnets have lower coercivity.

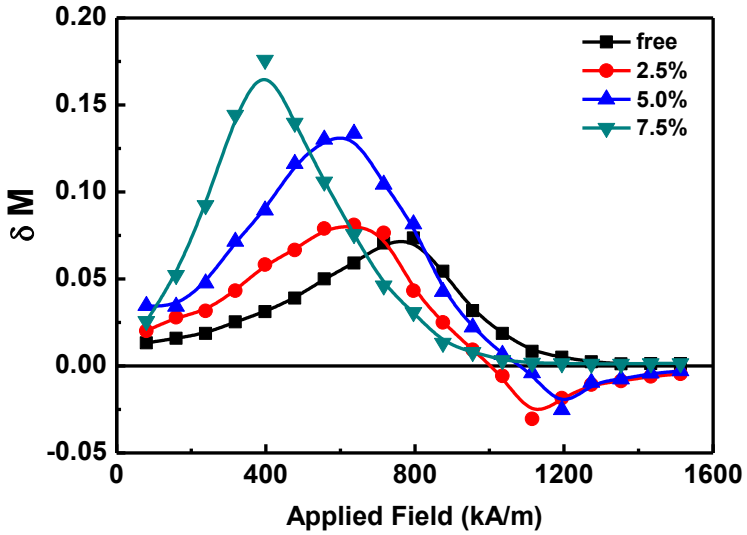

Figure 4. Variation of δm for the $SmCo_5$/α-Fe nanocomposite magnets with different α-Fe contents.

In order to qualitatively determine the intensity of exchange coupling effect in the nanocomposite magnets, the plots of $M(H)$ and $M_d(H)$ were investigated in the insets of Fig. 3. Here, $M_d(H)$ is defined as the remanence acquired after dc saturation in one direction. H_c is intrinsic coercivity defined by the condition for the magnetization $M(H_c)$=0, H_r is the dc field defined by the $M_d(H_r)$=0. It is found that the ratio of H_r/H_c is increased first and decreased subsequently with

increment of α-Fe content, are 1.21, 2.81, 1.59, 1.53 for 0, 2.5, 5, 7.5 wt% α-Fe, respectively. The latter values with more α-Fe are closer to the theoretical value predicted by Wohlfarth[16] (H_r /H_c=1.09), which is based on the model of randomly oriented uniaxial particles. It means that the samples with more α-Fe content is close to the model that the soft-magnetic phase (α-Fe) and the hard-magnetic phase ($SmCo_5$) obtain an uniform inverse under the applied field, resulting in it has a strong exchange-spring interaction.

For a better understanding the magnetic exchange interactions for the $SmCo_5$/α-Fe nanocomposite magnets, the exchange coupling interaction between the grains was analyzed by using the δM plot, which is defined as $\delta M(H)=[M_d(H)-M_r+2M_r(H)]/M_r$. Here, the $M_d(H)$ is reduced demagnetization remanence, and the $M_r(H)$ is reduced remanence magnetization[17,18]. The δM -H curves for the $SmCo_5$/α-Fe nanocomposite magnets with different α-Fe contents are presented in Fig. 4. It can be seen that a positive δM is obtained for all samples, confirming the existence of exchange coupling interaction between soft and hard phases. Meanwhile, a larger positive value of δM is obtained with more α-Fe content, compared with α-Fe free sample, indicating that the exchange coupling interaction is enhanced and finally enhancing the magnetic properties with α-Fe added. Similar behavior was observed by Rong et al. previously [19]. It should be noted the results of the δM are not all consist of the results of the H_r /H_c, the variance may be attributed to the varied magnetic analysis mechanisms.

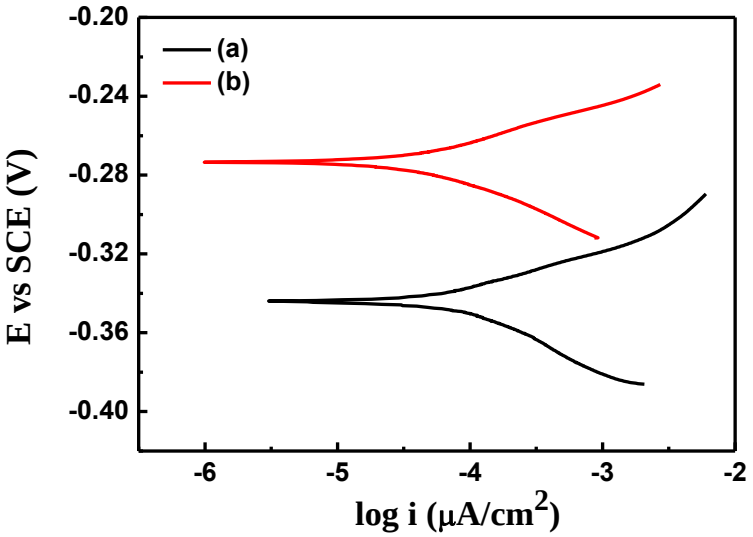

Figure 5. Polarization curves of the $SmCo_5$/α-Fe alloys with the α-Fe content at (a) free and (b) 7.5 wt% in 2.5 wt.% NaCl solution.

Fig. 5 shows the potentiodynamic polarization curves of the $SmCo_5$/α-Fe nanocomposite magnets for the α-Fe content at (a) free and (b) 7.5 wt% tested in 2.5 wt.% NaCl aqueous solutions. According to the potentiodynamic polarization curves, the corresponding corrosion potential E_{corr}, corrosion current density i_{corr} and Tafel slope b were obtained and showed in Table 1. The corrosion current density of the α-Fe free alloy is 97.72 μA/cm^2 derived from Tafel curve and the corrosion potential is -0.345 V. For the 7.5 wt% α-Fe content alloy, the corrosion current density decreases to 31.60 μA/cm^2 and the corrosion potential increases to -0.273 V. Furthermore, the Tafel slope b

behavior of the two alloys was calculated. Compared with α-Fe free sample, anodic Tafel slope *b* is decreased from 57.71 mV/dec to 40.40 mV/dec; cathodic Tafel slope *b* is also decreased from 62.49 mV/dec to 32.49 mV/dec. The lower values of corrosion current density i_{corr}, corrosion potential E_{corr} and Tafel slope *b* of the $SmCo_5$/α-Fe nanocomposite magnet with 7.5 wt% α-Fe content mean that electrochemical stability and corrosion resistance of the $SmCo_5$ magnet are remarkably improved by the addition of α-Fe.

Table 1. The corrosion potential E_{corr}, corrosion current density i_{corr} and Tafel slope *b* (anodic and cathodic) of the $SmCo_5$/α-Fe nanocomposite magnets for the α-Fe content at free and 7.5 wt% in 2.5 wt.% NaCl solution.

Alloys	E_{corr}(V)	i_{corr}(μA/cm^2)	*b*(mV/dec)	
			anodic	cathodic
free	-0.345	97.72	57.7	62.5
7.5 wt%	-0.273	31.60	40.4	32.5

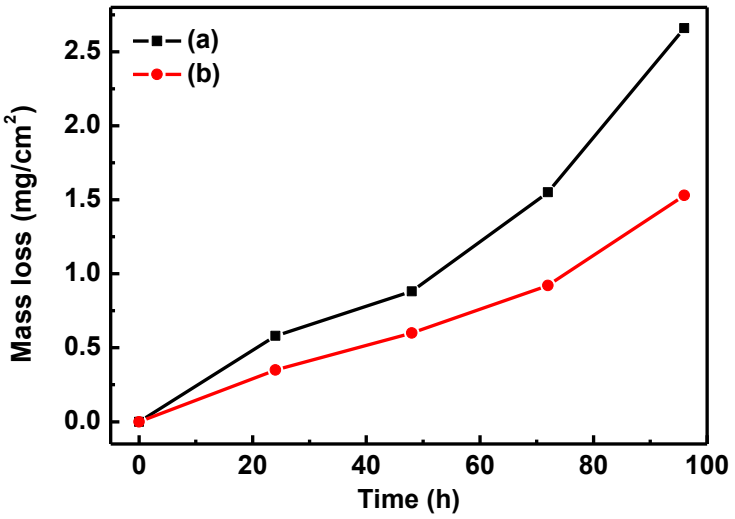

Figure 6. Mass loss of the $SmCo_5$/α-Fe nanocomposite magnets for the α-Fe content at (a) free and (b) 7.5 wt% under 120°C, 2 bar and 100% relative humidity atmosphere with different times.

The improvement of the corrosion resistance for the $SmCo_5$/α-Fe nanocomposite magnet with 7.5 wt% α-Fe content is also showed by the mass loss tests, as seen in Fig. 6 for the α-Fe free and α-Fe added magnets measured in 120°C, 2 bar and 100% relative humidity atmosphere for different times. With the increase of the exposure time, the mass loss of the two samples show the tendency of gradually increased. As the exposure time was prolonged to 96 h, the mass loss of the α-Fe free alloy reaches to ~2.66 mg/cm^2, compared to the $SmCo_5$/α-Fe nanocomposite magnet with the mass loss increase to ~1.53 mg/cm^2. The above results mean that the corrosion resistance of the $SmCo_5$/α-Fe nanocomposite magnet with 7.5 wt% α-Fe added can be improved in hot/humid atmosphere, which

may be the reason of the coexistence of hard and soft magnetic phases can enhance the oxidation and corrosion resistances.

The present study demonstrated that the magnetic properties can be improved and the exchange coupling interaction can be enhanced in the $SmCo_5$/α-Fe nanocomposite magnet with α-Fe added. Meanwhile, the corrosion resistance of these magnets can be also improved.

4. CONCLUSION

The influence of α-Fe content on the microstructure, magnetic properties and corrosion resistance of the $SmCo_5$/α-Fe nanocomposite alloys were investigated. The alloys that show strong exchange-coupling behavior ($(BH)_{max}$ = 11.3 kJ/m^3) was obtained when the α-Fe content at 7.5 wt%. The magnetization reversal results demonstrated that the α-Fe doped samples show low energy losses as a reversal field is applied, which is a big advantageous to the application in electrical machines and generators. Meanwhile, the corrosion resistance of these magnets can be also improved, with the lower corrosion current density i_{corr} (31.60 μA/cm^2), corrosion potential E_{corr} (-0.273 V) and Tafel slope b (anodic: 40.40 mV/dec, cathodic: 32.49 mV/dec).

ACKNOWLEDGEMENT
This work was supported by the National Natural Science Foundation of China (Grant No.51771176 and No. 51871205), and the Provincial Natural Science Foundation (LR15E010001).

References

1. R. Coehoorn, D.B. de Mooij, C. deWaard, *J. Magn. Magn. Mater*., 80 (1989) 101.
2. E.F. Kneller, R. Hawig, *IEEE Trans. Magn*., 27 (1991) 3588.
3. R. Skomski, J.M.D. Coey, *Phys. Rev. B*., 48 (1993) 15812.
4. H. Fukunaga, H. Nakamura, *IEEE Trans. Magn*., 36 (2000) 3285.
5. H. Fukunaga, H. Nakamura, *Scr. Mater*., 44 (2001) 1341.
6. J. Lee, T.Y. Hwang, M.K. Kang, G. Lee, H.B. Cho, J. Kim, Y.H. Choa, *Appl. Surf. Sci*., 471 (2019) 273.
7. D.Y. Feng, Z.W. Liu, G. Wang, Z.G. Zheng, D.C. Zeng, Z. Li, G.Q. Zhang, *J. Alloys Compd*., 610 (2014) 341.
8. M.I. Qadeer, B. Azhdar, M.S. Hedenqvist, S.J. Savage, *Prog. Org. Coat*., 76 (2013) 94.
9. Y.Y. Feng, L. Lou, M. Li, W.P. Song, T.H. Li, Y.X. Hua, X.H. Li, X.Y. Zhang, *J. Alloys Compd*., 744 (2018) 104.
10. P. Saravanan, M. Premkumar, A.K. Singh, R. Gopalan, V. Chandrasekaran, *J. Alloys Compd*., 480 (2009) 645.
11. Z.W. Liu, D.C. Zeng, R.V. Ramanujan, X.C. Zhong, H.A. Davies, *J. Appl. Phys*., 105 (2009) 07A736.
12. P.Y. Zhang, R. Hiergeist, L. Lüdke, M. Albrecht, H.L. Ge, *J. Appl. Phys*., 108 (2010) 043905.
13. D. Goll, M. Seeger, H. Kronmüller, *J. Magn. Magn. Mater*., 185 (1998) 49.
14. S.Y. Zhang, H.W. Zhang, B.G. Shen, *J. Appl. Phys*., 87 (2000) 1410.
15. C.Y. Hu, M.X. Pan, Q. Wu, H.L. Ge, X.M. Wang, Y.C. Lu, P.Y. Zhang, *J. Rare. Earth*., 34 (2016) 61.
16. E.P. Wohlfarth, *J. Appl. Phys*., 29 (1958) 595.

17. P. E. Kelly, K. O'Grady, P.I. Mayo, R.W. Chantrell, *IEEE Trans. Magn*., 25 (1989) 3881.
18. Q. Wu, A.R. Yan, H.L. Ge, P.Y. Zhang, X.K. Hu, Y. H. Liu, *J. Appl. Phys.*, 109 (2011) 07A739.
19. C.B. Rong, Y. Zhang, M.J. Kramer, J.P. Liu, *Phys. Lett. A*., 375 (2011) 1329.